Novel insights into old anticancer drugs

Zanden, S.Y. van der

Synthetic (*N,N*-dimethyl) doxorubicin glycosyl diastereomers to dissect modes of action of anthracycline anticancer drugs

5

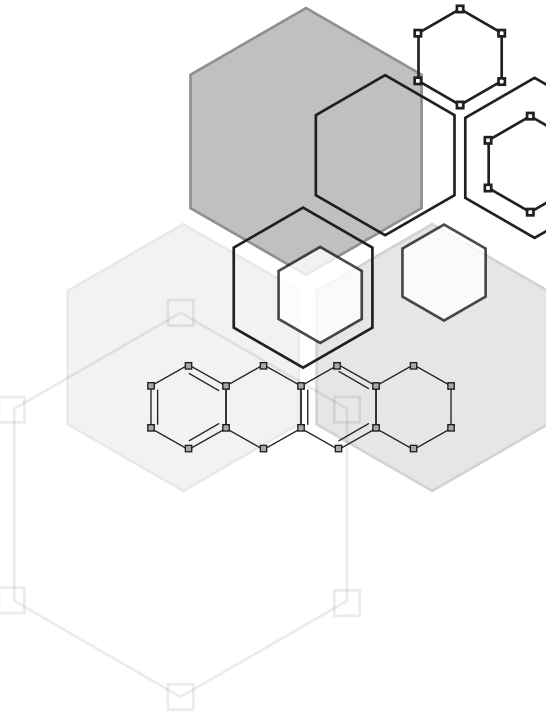

Sabina Y. van der Zanden[#], Dennis P.A. Wander[#], Merijn B.L. Vriends, Branca C. van Veen, Joey G. C. Vlaming, Thomas Bruyning, Gijsbert A. van der Marel, Jeroen D.C. Codee, Heman S. Overkleeft and Jacques Neefjes

[#]These authors contributed equally

Manuscript in preparation

ABSTRACT
Anthracyclines are effective drugs in the treatment of various cancers, but their use coincides with severe side effects. The archetypal anthracycline drug, doxorubicin, displays two molecular modes of action: DNA double strand break formation (through topoisomerase IIα poisoning) and chromatin damage (via eviction of histones). These biological activities can be modulated, and toxic side effects reduced by separating these two modes of action, through alteration of the aminoglycoside moiety of doxorubicin. Here, we report on the design, synthesis and evaluation of a coherent set of configurational doxorubicin analogs featuring all possible stereoisomers of the 1,2-amino-alcohol characteristic for the doxorubicin 3-amino-2,3-dideoxyfucoside, each in non-substituted and *N,N*-dimethylated forms. We show that both stereochemistry of the 3-amine carbon and *N*-substitution state are critical for anthracycline cytotoxicity and generally improve cellular uptake. *N,N*-dimethylepirubicin is identified as the most potent anthracycline that does not induce DNA damage while remaining cytotoxic.

INTRODUCTION
The anthracycline drug doxorubicin (adriamycin, Figure 1A, **1a**) is one of the most used anticancer drugs in history, and is annually subscribed to over one million cancer patients [1]. While doxorubicin is effective against a wide variety of tumors, including leukemia, non-Hodgkin's lymphoma and breast cancer, its use is limited by severe side-effects. Cardiotoxicity, the main treatment-limiting side effect, emerges in a cumulative manner, and for this reason treatment with doxorubicin is restricted to a maximum of six to eight treatment courses [2]. With the aim to identify more effective anthracyclines with limited side-effects, thousands of analogs of doxorubicin, either isolated from natural sources, produced by mutant enzymes or prepared by organic (semi) synthesis, have been evaluated in the past decades [3–5]. Only a handful of these anthracyclines has however entered the clinic. The 4'-epimer of doxorubicin, epirubicin (Figure 1A, **2a**) is one such clinically approved doxorubicin variant, in part because it appears to be effective at lower doses compared to doxorubicin for certain cancers, resulting in reduced cardiotoxicity [6]. Today, epirubicin is used in the treatment of breast-, ovarian-, gastric- and lung tumors, as well as several lymphomas [7]. This illustrates that new effective and less toxic anthracyclines can be developed, which may allow more intense, longer, and more effective treatment with limited long-term side effects for cancer survivors.
Understanding the molecular mode of action of anthracycline drugs is key for the development of new and improved (in terms of efficacy and toxicity) analogs. One key feature of doxorubicin is the formation of DNA double strand breaks due to topoisomerase IIα poisoning [8,9]. Doxorubicin inhibits topoisomerase IIα after the generation of DNA double stranded breaks and before re-ligation of DNA, thus resulting in DNA damage. For decades, this mode of action has been considered the main mechanism for the remarkable anticancer activity of doxorubicin and its structural analogs. However, aclarubicin (Figure 1B), another anthracycline analog used in Japan and China, is at least equally effective in the treatment of acute myeloid leukemia (AML), but does not produce such DNA double stranded breaks [9]. Moreover, aclarubicin is much less cardiotoxic [10]. We recently showed the existence of a second activity of anthracyclines: eviction of histones from the chromatin [9]. These evicted histones are then replaced by new nascent ones, resulting in epigenetic alterations [11]. Further, we showed that histone eviction combined with

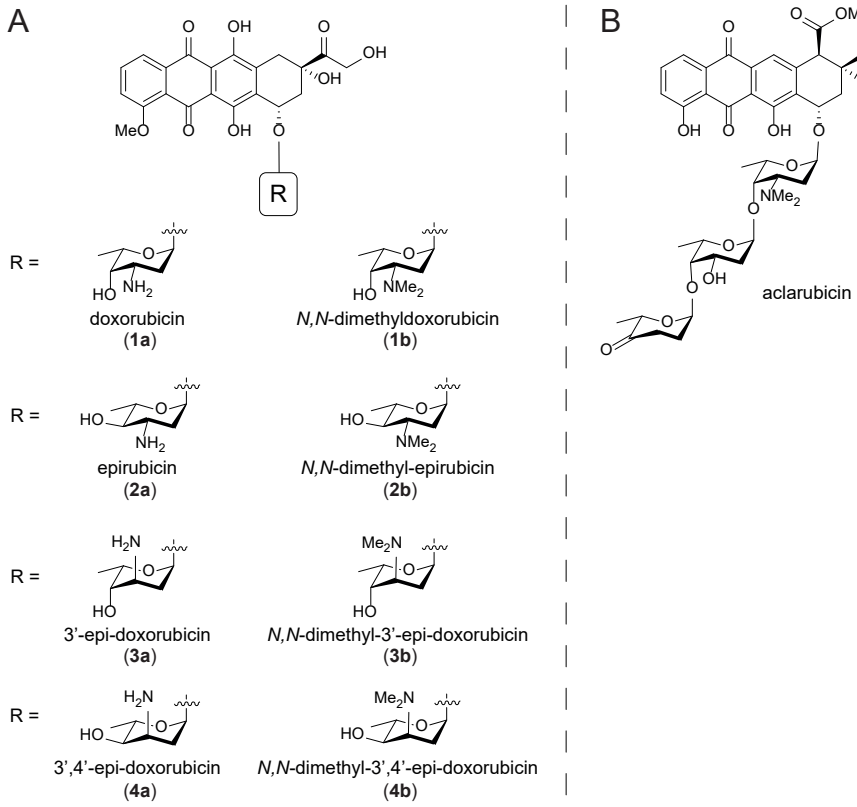

Figure 1. Chemical structures of doxorubicin and analogs. *(A) doxorubicin (**1a**) and derivatives (**1b**-**4b**), differing in stereochemistry and N,N-dimethylation on the sugar moiety. (B) structure of aclarubicin.*

DNA double strand break formation, as for doxorubicin, is responsible for the major side effects of doxorubicin; cardiotoxicity and secondary tumor formation [10]. In this study, we showed that *N,N*-dimethyldoxorubicin (Figure 1, **1b**), a close doxorubicin analog featuring the dimethylamine characteristic for aclarubicin, mirrors the biological activity of aclarubicin, by only inducing histone eviction [10]. Like aclarubicin, *N,N*-dimethyldoxorubicin is an effective anticancer agent and lacks the severe side effects displayed by doxorubicin in various mouse models [10]. These data show that chemically separating DNA- from chromatin damage activities, as found in the anthracyclines currently used in the clinic, results in drugs lacking the major long-term side effects. In addition, chromatin damage appeared to be the major cause for the anticancer activity of these compounds. Our follow-up studies on a series of doxorubicin/aclarubicin hybrid structures, varying in the tetracyclic aglycon, the sugar moiety (from monosaccharide as in doxorubicin up until the aclarubicin trisaccharide) and the *N*-alkylation pattern confirm previous results that dimethylated structures fail to induce DNA double strand breaks while remaining cytotoxic [12]. This work raises the question if there is a structure-activity relationship for stereoisomeric analogs of doxorubicin, and whether this may lead to potential new effective

anticancer drugs. To test this, we synthesized and evaluated a coherent, focused library of epimeric doxorubicin analogs featuring entries of all four stereoisomeric forms of the 1,2-amino alcohol arrangement of the 3-amino-2,3-dideoxy-L-fucoside (daunosamine) characteristic for doxorubicin (**1a**). Each of these entries features the non-substituted as well as the *N,N*-dimethylated compound. Together, this resulted in the synthesis of compounds **1a/b** - **4a/b** (Figure 1), some of which have been reported previously [10,13,14].
Here we report a general synthesis route for the preparation of these target compounds, based on the use of gold-catalyzed glycosylation reactions of alkynylbenzoate donors. Most of these proceed with excellent stereoselectivity, which can be related to the oxocarbenium ion intermediates formed in these reactions. Subsequently, we evaluated the biological activities of the systematic set of diastereoisomers by dissecting their capacity to induce DNA damage, histone eviction, their cellular uptake and cytotoxicity. Dimethylation of the sugar amine and an equatorial orientation of this moiety are required for cytotoxicity of these compounds and generally improve cellular uptake *in vitro*. These features are combined in *N,N*-dimethylepirubicin (**2b**), the most potent anthracycline in this coherent set of epimeric doxorubicin analogs, which has an excellent cytotoxicity profile with only chromatin damage activity.

RESULTS AND DISCUSSION

Synthesis of a coherent set of (*N,N*-dimethyl)doxorubicin sterioisomers.

We started with the development of synthetic methodology to prepare the focused library depicted in Figure 1A (compounds **2b**, **3a/b**, **4a/b**). Recently, we reported on the synthesis of *N,N*-dimethyldoxorubicin (**1b**) [10], whereas doxorubicin (**1a**) and epirubicin (**2a**) are both commercially available. Our methodology is rooted in gold(I)-mediated glycosylation chemistry, developed by Yu and coworkers [15], that in our hands has proven effective in the creation of the anthracycline α-fucosidic linkages [12,16]. In the assembly of doxorubicin/aclarubicin hybrids we found that the use of an allyloxycarbonate to mask the amino group of the 2,3-dideoxy-3-aminofucose in combination with relatively labile silyl ethers to protect the hydroxyl groups proved very effective for the assembly of the anthracycline targets and we therefore adopted this protecting group strategy here as well [12]. Thus, alkynylbenzoate donors **9**, **12** and **16** were designed and assembled as depicted in Scheme 1. *p*-Methoxyphenolates **6** and **10** were prepared from precursor **5** [17] (a mixture of 33 : 67 R/S at C3) by treatment with *p*-methoxyphenol in the presence of catalytic TMSOTf to give α-configured equatorial azide **6** in 50% yield and β-configured axial azide **10** in 7%. Deacylation under Zemplén conditions was followed by triethylsilylation, and the azide was then converted to the allyloxycarbamate using a Staudinger reduction, after which reaction of the liberated amine with allylchloroformate gave fully protected **7** and **11**. The *p*-methoxyphenolates were then subjected to oxidative hydrolysis of the anomeric *p*-methoxyphenolate using $Ag(DPAH)_2$) [18], delivering the lactols which were transformed into the required alkynylbenzoates (ABz) by a Steglich esterification with o-cyclopropylethynylbenzoic acid **8** [19], providing donor glycosides **9** and **12**.
In preparing for the synthesis of the 3-*epi*-daunosamine donor **16**, acetate **13** [20], was converted to the *p*-methoxyphenolate by the action of $BF_3{\cdot}OEt_2$ giving, after deacylation, compound **14**. Triethylsilylation of the 4-hydroxyl and conversion of the azide into the allyloxycarbamate yielded **15**. Removal of the anomeric *p*-methoxy-

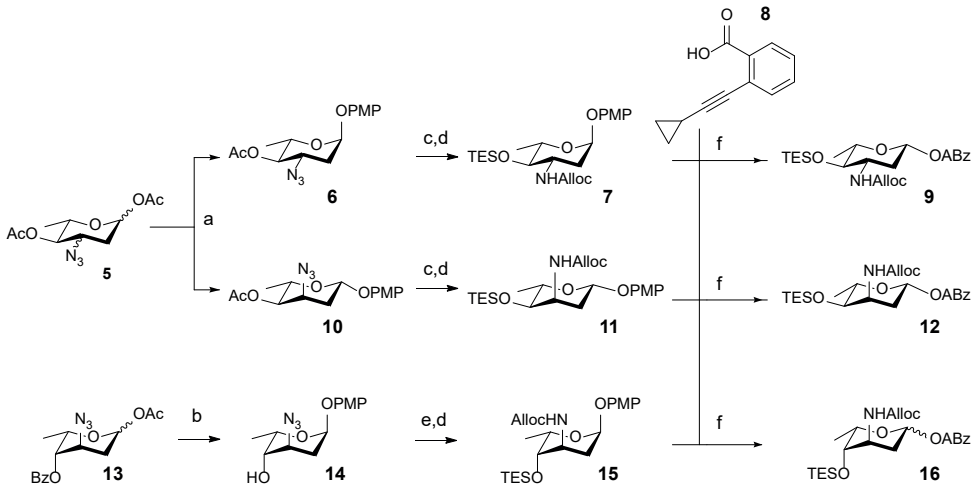

Scheme 1. Synthesis of aminosugar alkynylbenzoate donors 9, 12 and 16. *Reagents and conditions: (a) p-methoxyphenol, TMSOTf, DCM, 0°C, 50% for 6, 7% for 10; (b) i. p-methoxyphenol, $BF_3{\cdot}OEt_2$, DCM, -60°C to -40°C; ii. NaOMe, MeOH, 70% over 2 steps; (c) i. NaOMe, MeOH; ii. TESOTf, pyr., DCM, 95% over 2 steps from 6, quant. from 10; (d) i. polymer-bound PPh_3, THF, H_2O; ii. allyl chloroformate, pyr., DCM, quant. over 2 steps for 7; 95% over 2 steps for 11; quant. over 2 steps for 15; (e) TESOTf, pyr., quant.; (f) i. $Ag(DPAH)_2$, H_2O, NaOAc, MeCN, H_2O, 0°C; ii. EDCI·HCl, DMAP, DIPEA, DCM, 49% over 2 steps for 9 (β-anomer only), 57% over 2 steps for 12 (β-anomer only), 79% over 2 steps for 16 (1:3 α:β).*

phenol group and installation of the alkynylbenzoate was then achieved as described for donors **9** and **12** to give donor **16**. The three alkynylbenzoate donors **9**, **12** and **16** were used, alongside daunosamine donor **17** that we previously assembled [12], in glycosylation reactions towards doxorubicin analogs **2b** - **3a/b** - **4a/b** (Scheme 2). Treatment of a mixture of donor **9** and protected doxorubicinone acceptor **18** [21], with a catalytic amount of PPh_3AuNTf_2 in DCM at room temperature led to the formation of anthracycline **19** in 80% yield as an 8:1 α:β-mixture. The desired α-anomer could be readily separated to provide the desired axially linked **19**. The analogous glycosylation of **12** and **18** proceeded with poor stereoselectivity and provided **20** as a 1.5:1 α:β mixture in 50% yield. The condensation of donor **16**, having two axial substituents at C-3 and C-4, led to the formation of the protected doxorubicin analog **21** with excellent stereoselectivity and the desired product was obtained as a single anomer in 58% yield. The glycosylation of daunosamine donor **17** and **18** also delivered the desired α-anomer with excellent stereoselectivity, forming **22** in 54% yield. We suggest that the observed stereoselectivity - or lack thereof - in these glycosylations can be understood upon perusal of the intermediate oxocarbenium ions (or oxocarbenium ion-like species), their conformational behavior and the direction nucleophiles may take towards forming a glycosidic linkage. The dideoxy nature of the used donors makes them relatively reactive ('armed') and the anomeric cation thus readily forms upon activation of the alkynylbenzoate anomeric leaving group.‡ The intermediate oxocarbenium ion can adopt different conformations (often close to half-chair structures) and preferred conformations are the result of stereoelectronic effects of the substituents on the ring [22]. Electronegative atoms (such as oxygen and nitrogen) prefer to adopt an axial orientation when mounted at C-3 or

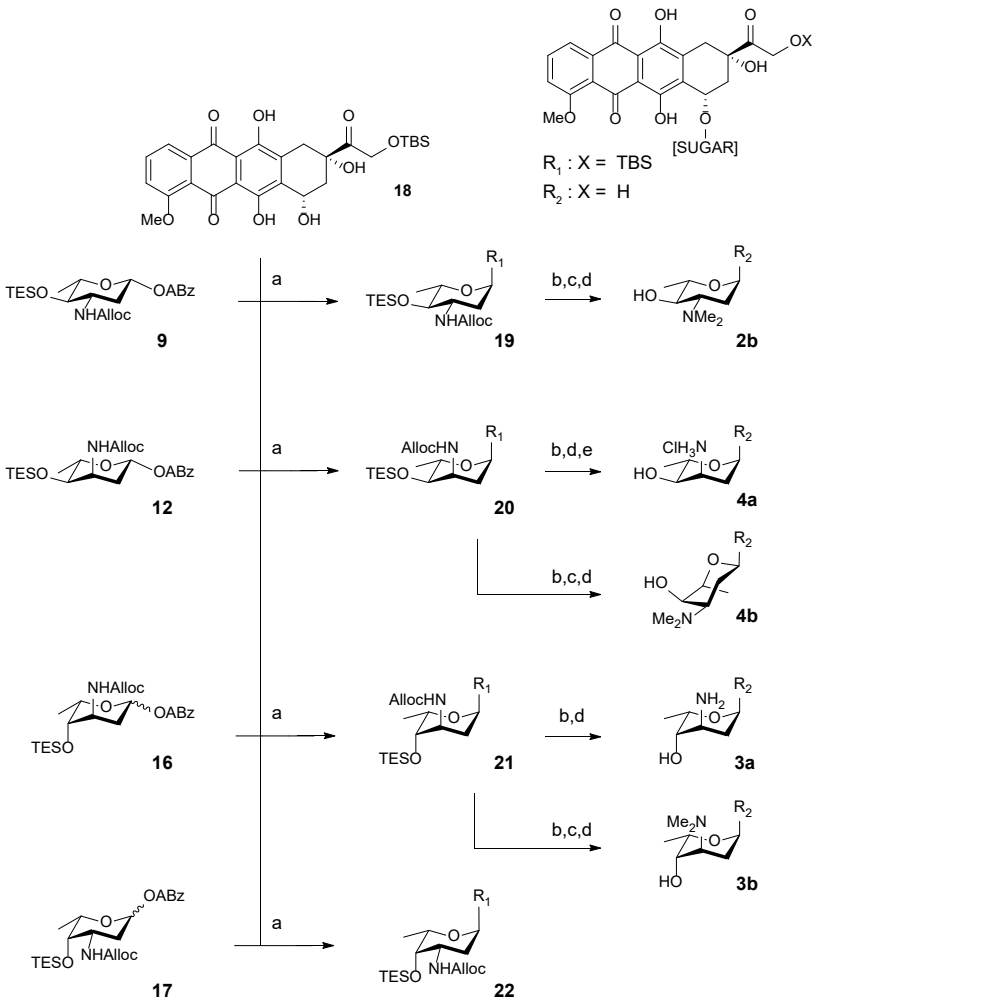

Scheme 2. Synthesis of (*N,N*-dimethyl)doxorubicins 2b - 3a/b - 4a/b. *(a) 10 mol% PPh_3AuNTf_2, DCM, 80% for 19 (8:1 α:β); 50% for 20 (1.5:1 α:β); 58% for 21 (>20:1 α:β), 54% for 22 (>20:1 α:β); (b) $Pd(PPh_3)_4$, NDMBA, DCM, 82% from 19; (c) $NaBH(OAc)_3$, aq. CH_2O, EtOH, 82% from 19; 72% over 2 steps from 20; (d) HF·pyr., pyr., 0°C, 83% for 2b; 35% over 3 steps for 4b; 72% over 2 steps for 3a, 66% for 3b; (e) lyophilization from aq. HCl, 54% over 3 steps.*

C-4. Alkyl groups will preferentially adopt a *pseudo*-equatorial orientation for steric reasons [22–24]. In addition, an incoming nucleophile, that will preferentially attack this oxocarbenium ion from the β-face (to deliver the product through a favorable chair-like transition state), will experience 1,3-diaxial interactions with the substituent at C-3 as well as the C-6 methyl group. Therefore, the incoming doxorubicinone nucleophile will preferentially attack the all-equatorial 3H4 conformer of **9**, leading to the formation of the α-product in good selectivity (Scheme 3A). The $^3H_4$ and $^4H_3$ half chair oxocarbenium ions that emerge from activating donor **12** each place one of the electronegative substituents in an axial position, and will therefore be of comparable

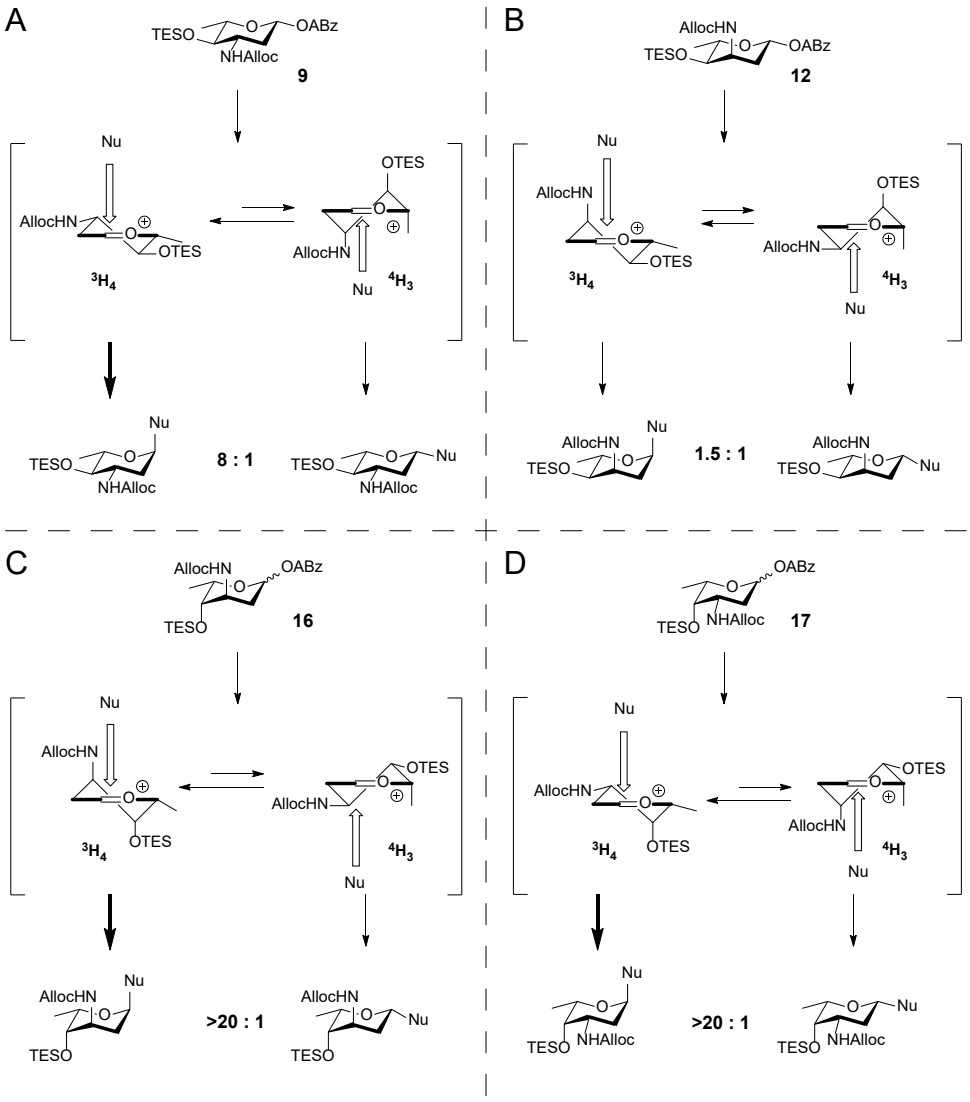

Scheme 3. Mechanistic rationale for the stereoselectivity found in the glycosylations of donors 9, 12, 16 and 17 with acceptor 18. *The equilibria between the $^3H_4$ and $^4H_3$ conformers of the oxocarbenium ions are indicated. The bold arrows indicate the most favorable product forming pathways. Nu = acceptor **18**.*

stability (Scheme 3B). The trajectories of incoming nucleophiles on these ions will experience similar steric interactions, explaining the poor selectivity observed in the glycosylation of donor **12** and acceptor **18**. Zeng et al. have previously reported that glycosylations of similar ristosaminyl alkynylbenzoate donors to various glycosyl acceptors proceeded with comparably poor selectivity [25]. The excellent stereoselectivity of donor **16** can be traced back to the $^3H_4$ half chair oxocarbenium ion, which places both the C-3 and C-4 electronegative groups in an axial position, while having the C-6-methyl oriented equatorially (Scheme 3C). This ion is preferentially attacked

from the top face to provide the α-linked product. Finally, when the half chair ions formed from daunosamine donor **17** are regarded, the $^{3}H_{4}$ one appears the most favorable, because it benefits from the axially oriented C-4-OTES group and lacks unfavorable 1,3-diaxial interactions (Scheme 3D). In addition, the incoming nucleophile will experience little steric interactions when approaching this ion from the top face, explaining the excellent stereoselectivity of donor **17**.
With the fully protected anthracyclines in hand we focused on deprotection of the compounds and the installation of the methyl groups on the amines (Scheme 2). Deblocking of the Alloc carbamate in **19** was achieved by treatment with catalytic $Pd(PPh_3)_4$ in the presence of *N,N*-dimethylbarbituric acid (NDMBA) [26] as the allyl scavenger to liberate the amine. Reductive amination using formaldehyde and a stoichiometric amount of $NaBH(OAc)_3$, was followed by desilylation with HF in pyridine to afford target compound *N,N*-dimethylepirubicin **2b**. Alloc removal of **20** and subsequent desilylation delivered **4a**, which was turned into its HCl salt for solubility. Reductive amination of the amine formed upon Alloc removal from **20** and desilylation delivered **4b**. Using a similar sequence of reactions, **21** was transformed into **3a** and **3b**. Of note, NMR analysis of compound **4b** indicated that the sugar ring adopts a $^{4}C_{1}$ conformation, rather than the $^{1}C_{4}$ conformation, taken up by its non-methylated counterpart **4a** (see supplemental information Figure S4 for annotated NMR spectra). The observed conformation of the L-megosamine sugar moiety in **4b** is consistent with that found in the macrolide megalomycin [27]. As a result, the tertiary amine in **4b** points away from the aglycone, and the overall shape of anthracycline **4b** differs significantly from the other generated compounds.

Biological evaluation of (*N,N*-dimethyl)doxorubicin sterioisomers
Doxorubicin and its analogs used in the clinic, have two main activities: DNA damage and chromatin damage [9,10]. Modification at the amine can separate these activities, but sugar epimers of doxorubicin have not been evaluated for this. Therefore, we assessed our panel of (*N,N*-dimethyl)doxorubicin isomers for these biological activities. DNA double strand break formation by the various compounds was determined (indirectly) by visualization of γH2AX (a post-translational modification on histone H2A that occurs as part of the DNA damage response) by western blot analysis (Figure 2A and B) [28]. In addition, DNA breaks were assessed more directly using constant-field gel electrophoresis (CFGE) (Figure 2C and D). The anthracyclines bearing a free amine in their sugar, i.e. doxorubicin (**1a**), epirubicin (**2a**), 3'-epi-doxorubicin (**3a**) and 3',4'-epi-doxorubicin (**4a**) all induced DNA breaks. For the analogs featuring a tertiary amine (**1b**, **2b**, **3b** and **4b**), DNA double strand break formation was absent or reduced, compared to their primary amine counterparts. *N,N*-dimethyldoxorubicin (**1b**) and *N,N*-dimethyl-epi-doxorubicin (**2b**) induced (almost) no DNA breaks, yet *N,N*-dimethyl-3'-epi-doxorubicin (**3b**) and *N,N*-dimethyl-3',4'-epi-doxorubicin (**4b**) did produce DNA breaks, although significantly less so than their non-methylated counterparts (Figure 2B and D). Overall, the orientation of the 4-OH function (**1a** vs **2a**, **1b** vs **2b**, **3a** vs **4a**, **3b** vs **4b**) had little effect on their DNA damaging activity. Since our previous findings indicate that chromatin damage, rather than DNA damage, is the most dominant cytotoxic mechanism of tumor killing by anthracycline drugs [10,11], we investigated the ability of our panel of compounds (**1a/b** - **4a/b**) to induce histone eviction. To do so, part of the nucleus of MelJuSo cells stably expressing PAGFP-H2A was photoactivated, and release of these fluorescent histones was followed over time upon treatment with the different compounds (Figure 3A and supplemental information Figure S1). In all cases, the *N,N*-dimethylated variants (**1b**, **2b**, **3b** and

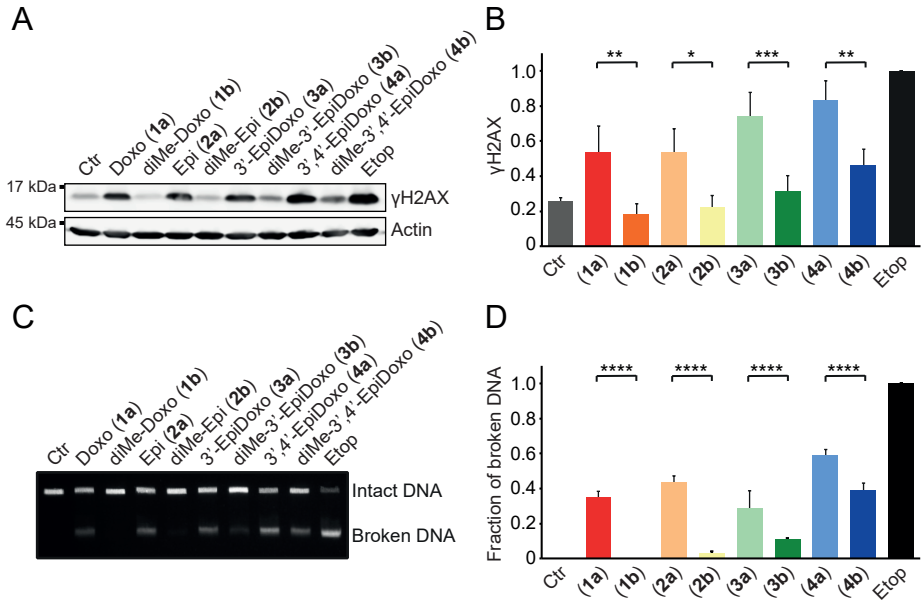

Figure 2. DNA damage formation by the epimeric doxorubicin analogs (1a/b - 4a/b). *K562 cells were treated for 2 hours with 10μM of the indicated compounds, and etoposide (10 μM) was used as a positive control. (A) DNA double strand breaks were measured indirectly by visualization of the γH2AX levels by Western blot. Actin was used as a loading control and molecular weight markers are indicated. (B) Quantification of the γH2AX signal normalized to actin, and relative to etoposide. Results are presented as mean ± SD of three independent experiments. Ordinary one-way ANOVA; *P < 0.05, **P < 0.01, ***P < 0.001. (C) DNA break formation by the various compounds was directly analyzed by CFGE. The position of intact and broken DNA is indicated. (D) Quantification of the fraction of broken DNA relative to etoposide. Results are presented as mean ± SD of four independent experiments. Ordinary one-way ANOVA; ****P < 0.0001.*

4b) were more potent in evicting histones than their free amine counterparts (Figure 3A). Of the dimethylated compounds, *N,N*-dimethyl-3'-epidoxorubicin (**3b**) showed the lowest histone evicting activity and 3'-epidoxorubicin (**3a**) was the only compound that failed to evict histones. Subsequently, the cytotoxicity of the compounds was determined in a panel of 14 different tumor cell lines *in vitro* (Figure 3B and 3C, and supplemental information Figure S2). With the exception of compound **3b**, all compounds with tertiary amines have a lower IC_{50} value in the tested tumor cell lines than their non-methylated counterparts. Furthermore, the compounds with the amine in an equatorial position (**1a/b**, **2a/b** and **4b**) are effective at killing most of the tumor cell lines, down to nanomolar concentrations, while the compounds with the amine in axial configuration (**3a/b**, **4a**) show poor cytotoxicity. The difference in cytotoxicity between **3a** versus **4a**, and **3b** versus **4b** is remarkable. 3'-Epidoxorubicin (**3a**) and 3',4'-epidoxorubicin (**4a**) both show poor cytotoxicity and the dimethylated variant of **3a**, compound **3b**, is not more effective, while the dimethylated variant of **4a**, being **4b**, is significantly more cytotoxic (Figure 3C). Possibly, this is due to the fact that the sugar in *N,N*-dimethylated **4b** exists in a different conformation than in **4a**, placing the C-3 dimethylamino group in an equatorial orientation (similarly to **1a/b** and **2a/b**), pointing away from the aglycone rather than towards it (as for compounds **3a/b** and

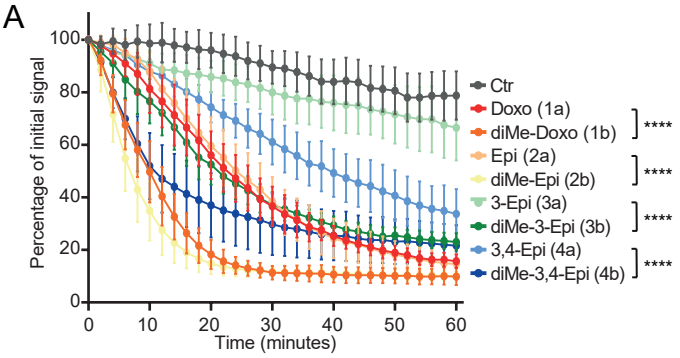

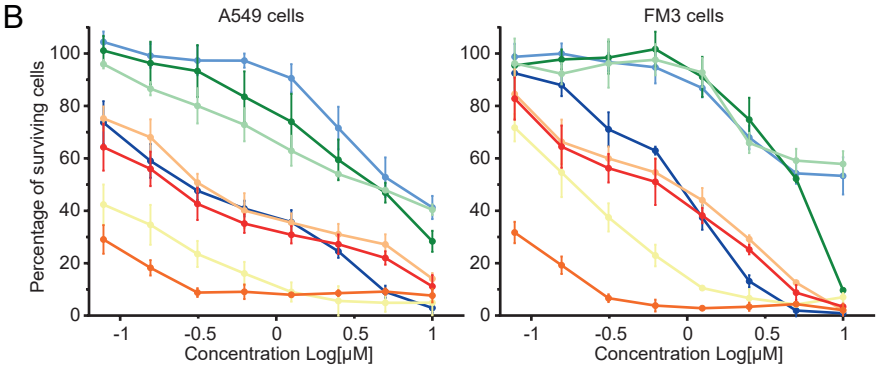

C

Cells \ Drugs [μM]	Doxo (**1a**)	diMe-Doxo (**1b**)	Epi (**2a**)	diMe-Epi (**2b**)	3-Epi (**3a**)	diMe-3-Epi (**3b**)	3,4-Epi (**4a**)	diMe-3,4-Epi (**4b**)
A549	0.226	0.006	0.455	0.053	3.996	3.942	6.347	0.328 ****
BT474	4.106	0.355	3.692	0.428	6.906	10.720	7.721	1.669 ****
BXPC3	3.161	0.135	3.460	0.333	N.D.	N.D.	N.D.	1.480 ****
DU145	0.531	0.190	0.643	0.198	6.759	4.422	6.093	0.273 ****
FM3	0.501	0.039	0.623	0.189	10.820	4.604	8.395	0.765 ****
HCT116	0.514	0.042	0.441	0.158	3.948	4.513	4.646	0.423 ****
Hela	0.108	0.016	0.096	0.085	0.899	1.867	1.207	0.160 ****
K562	0.230	0.122	0.184	0.070	2.117	1.778	1.571	0.229 ****
MelJuSo	0.393	0.046	0.246	0.136	1.853	3.825	1.825	0.286 ****
PC3	0.540	0.122	0.722	0.226	6.330	11.890	8.304	0.800 ****
SKBR3	1.301	0.248	1.101	0.302	7.581	4.136	7.158	0.569 ****
U2Os	0.191	0.028	0.287	0.095	3.997	3.908	2.945	0.385 ****
U87	0.291	0.006	0.314	0.132	7.663	6.523	5.905	0.608 ****
U118	1.379	0.074	1.644	0.109	N.D.	5.734	N.D.	0.568 ****

Figure 3. Chromatin damage capacity and cytotoxicity of epimeric doxorubicin analogs. *(A) Quantification of histone eviction measured as PAGFP-H2A release from photoactivated nuclear regions after administration of 10μM of the indicated doxorubicin isomers (in colors on right). Ordinary two-way ANOVA, Turkey's multiple comparison test; ****P < 0.0001. (B) Cytotoxicity of* ***1a/b*** *-* ***4a/b*** *in A549 and FM3 cells. Cells were treated for 2 hours with different concentration of the indicated isomers followed by drug removal. Cell survival was determined 72 hours post drug removal using CellTiter-Blue. Colors correspond to the drugs shown in Figure 3A. Data is shown as mean ± SD from 4 independent experiments.*

Figure 3. Continued. *(C) Color code table depicting the IC_{50} for compounds 1a/b - 4a/b determined for the 14 tumor cell lines tested. Red, (high IC_{50} = low cytotoxicity), to yellow (medium IC_{50}), to green (low IC_{50} = high cytotoxicity). IC_{50} for 4a vs 4b: Ordinary two-way ANOVA with Sidak's multiple comparison test; ****P < 0.0001.*

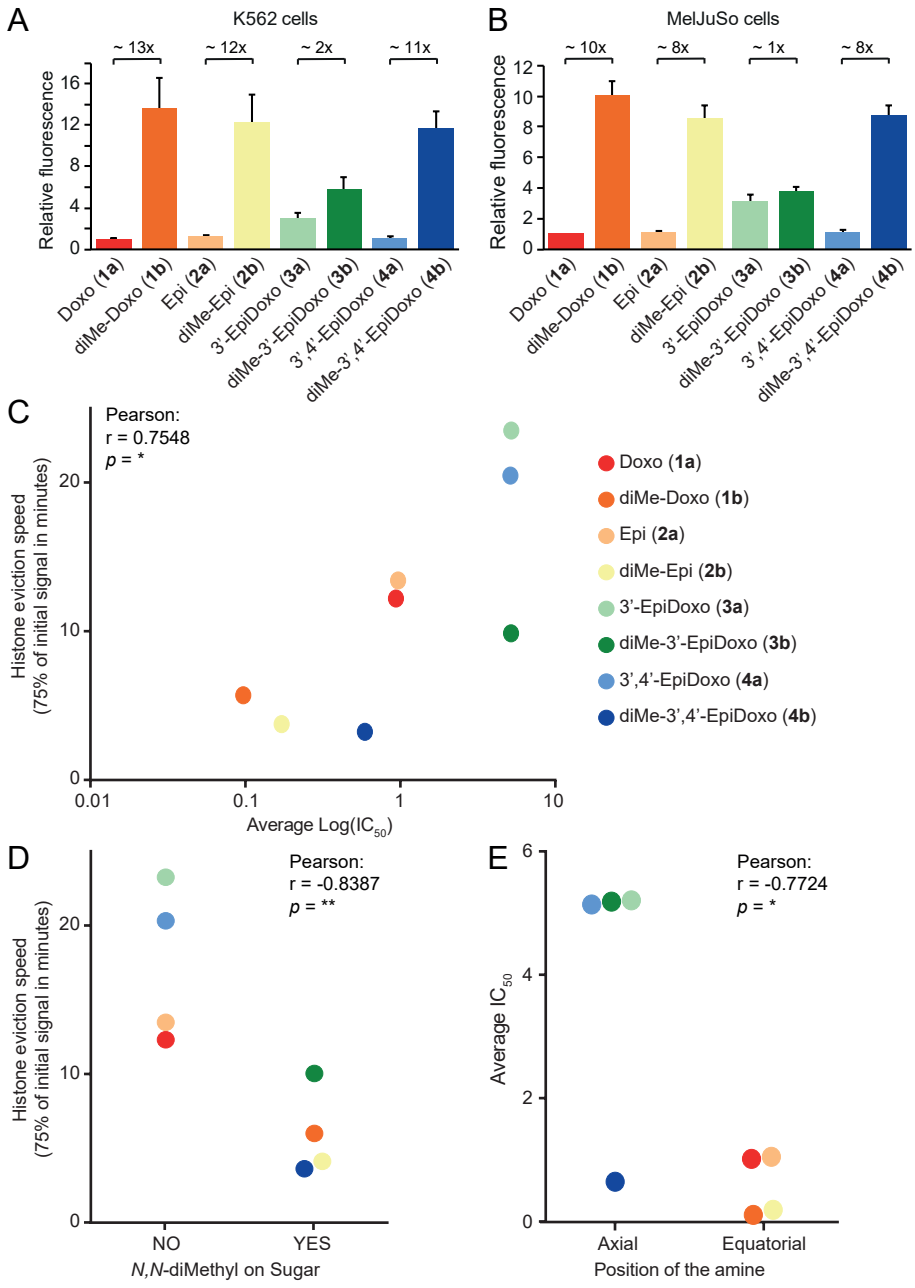

Figure 4. *See legend on next page.*

Figure 4. Structure-function relationship of our library of (*N,N*-)dimethyldoxorubicin isomers. *(A and B) Uptake of the different isomers 2 hours post treatment with 1μM of the indicated compound for K562 (A) and MelJuSo (B) cells. Relative fluorescence to the parental compound doxorubicin is plotted for K562 and MelJuSo cells. Data is shown as mean ± SD. (C) Histone eviction speed (the time at which 25% of the initial signal is reduced) is correlated with IC_{50} of the various doxorubicin isomers. (D) N,N-dimethylation of the sugar of the analogs enhances the histone eviction speed. (E) Equatorial positioning of the amine improves the cytotoxicity of the doxorubicin analogs. Two-tailed Pearson r correlation p = * < 0.05, ** < 0.01.*

4a). Another critical factor for the effectiveness of drugs is their ability to enter the cell. Since all variants in this library are fluorescent, this could be easily determined by flow cytometry. K562 and MelJuSo cells were treated with compounds **1a/b** – **4a/b** and intracellular fluorescence was measured 2 hours post treatment (Figure 4A and B). Compounds **1b**, **2b** and **4b** all featuring the *N,N*-dimethyl are taken up much more efficiently than the corresponding primary amines, **1a**, **2a** and **4a**, respectively. This was not the case for **3a**, which was already taken up more efficiently than the other primary amine epimers. The difference in uptake with its dimethylated variant **3b** is small. Overall, it can be concluded that the cytotoxicity of the here studied anthracyclines is mainly determined by their histone eviction effectivity (Figure 4C and supplemental information Figure S3A), which strongly correlates to the rate of uptake of the compounds (Figure 4A and B). Compounds featuring an *N,N*-dimethyl moiety are more effective histone evictors (Figure 4D) and are therefore more cytotoxic than the corresponding compounds having a primary amine, while the orientation of the OH group at the 4' position has very little effect on cytotoxicity (supplemental information Figure S3A and B). Additionally, the stereochemistry of the fucose-carbon (C-3) bearing the amine functionality has a major influence on the IC_{50} values of the compounds *in vitro*. Compounds featuring an equatorial amine are the most effective (**1a/b**, **2a/b** and **4b**; Figure 4E).

CONCLUSION

Despite the widespread use of doxorubicin in the clinic for the treatment of various cancers for several decades, its structure-activity relationship is still not fully understood. Although doxorubicin is a very effective anticancer drug, its use is limited by cumulative cardiotoxicity and treatment related secondary tumors. Chromatin damage by eviction of histones is a new mode of action of anthracyclines [9], which brings renewed interest to develop new doxorubicin analogs. We showed that the anthracyclines, *N,N*-dimethyldoxorubicin (**2b**) and aclarubicin, are unable to generate DNA breaks, yet induce chromatin damage via eviction of histones [10]. These compounds remain equally potent as doxorubicin, but without the induction of cardiotoxicity and secondary tumor formation. Here, we synthesized and tested a focused library of stereoisomers with respect to the 1,2-amino-alcohol characteristic for the daunosamine sugar within doxorubicin; and the four possible stereoisomers both as primary and tertiary (dimethylated) amines. Analysis of this focused library showed that doxorubicin isomers with the amine positioned axially have poor histone eviction activity and display limited cytotoxicity compared to their equatorial amine counterparts. The exception to this is **4b**, in which the sugar moiety has shown to undergo a ring-flip in solution. Possibly, this configuration, having an equatorial orientation of the amine as a result, causes the observed activities. Remarkably, the *N,N*-dimethylated variants showed strongly improved cellular uptake, some up to 10-fold, when compared to their non-methylated counterparts. How anthracyclines

are taken up by cells is unclear, but the *N,N*-dimethylation likely increases the basicity of the amine, and also the logP, both of which could influence diffusion over the hydrophobic cell membrane. The rate of histone eviction correlates strongly with the cellular uptake, which influences their cytotoxicity. Further chemical modifications of anthracyclines aimed at improving cellular uptake will help in achieving cytotoxicity at lower concentrations.
We have shown previously that *N,N*-dimethyldoxorubicin (**1b**) completely abolishes DNA double strand break formation while not affecting the ability to kill tumor cells, when compared to doxorubicin (**1a**), which does induce DNA damage [10]. This appears to be a general theme, as *N,N*-dimethylepirubicin (**2b**) also lacks DNA damage capacity and is more cytotoxic than epirubicin (**2a**). Because *N,N*-dimethylepirubicin (**2b**) displays potent anti-tumor activity *in vitro*, lacks DNA damage activity and therefore possibly also lacks cardiotoxicity and second tumor formation [10], it makes us believe this compound could be an attractive lead for further development towards novel, possibly more effective anthracyclines with limited side effects. More generally, we feel our results, based on the synthesis and evaluation of this focused library of close structural and stereochemical analogs, warrants the assessment of more such compound collections. These would feature, for instance, selected variations in the aglycon, in the sugar part (instead of stereoisomers as presented here also regio-isomers and/or glycosylated derivatives) and in the nature of the amine (next to methylation also other alkyl substituents). Evaluating the chemical space around old anticancer drugs can lead to the discovery of new activities and improvement of these drugs, as illustrated in this study.

MATERIALS AND METHODS

Chemicals

Doxorubicin and epirubicin were purchased from Accord Healthcare Limited, UK and etoposide from Pharmachemie, NL.

Cell Culture

K562 cells (B. Pang, Stanford University, USA), HCT116 cells (T. van Hall, LUMC, The Netherlands), BXPC-3 cells (ATCC® CRL-1687), PC3 and DU145 cells (C. Robson, Newcastle University, UK), were maintained in RPMI-1640 medium supplemented with 8% FCS. A549 cells (R. Bernards, NKI, The Netherlands), FM3 cells (D. Peeper, NKI, The Netherlands), U87 MG (ATCC® HTB-14), U118 MG (ATCC® HTB-15), U2Os cells (ATCC® HTB-96), Hela cells (ATCC® CCL-2) and SKBR3 (R. Beijersbergen, NKI, The Netherlands), were maintained in DMEM medium supplemented with 8% FCS. BT474 cells (R. Beijersbergen, NKI, The Netherlands) were maintained in DMEM/F12 medium supplemented with 8% FCS. MelJuSo cells were maintained in IMDM medium supplemented with 8% FCS. MelJuSo cells stably expressing PAGFP-H2A were maintained in IMDM supplemented with 8% FCS and G-418, as described. Cell lines were maintained in a humidified atmosphere of 5% CO_2 at 37°C and regularly tested for the absence of mycoplasma.

Western blot and constant-field gel electrophoresis (CFGE)

Cells were treated with drugs at indicated dose for 2 hours. Subsequently, drugs were removed by extensive washing and cells were collected and processed immediately for the assays. Cells were lysed directly in SDS-sample buffer (2%SDS, 10% glycerol, 5% β-mercaptoethanol, 60mM Tris-HCl pH 6.8 and 0.01% bromophenol

blue). Lysates were resolved by SDS-PAGE followed by Western blotting. Primary antibodies used for blotting: γH2AX (1:1000, 05-036, Millipore), β-actin (1:10000, A5441, Sigma). DNA double strand breaks were quantified by constant-field gel electrophoresis as described [29]. Images were quantified using ImageJ software.

Microscopy
PAGFP-H2A photoactivation and time-lapse confocal imaging were performed as described [9] on a Leica SP8 confocal microscope system, 63x lens, equipped with a climate chamber. Loss of fluorescence after different treatments was quantified using ImageJ software.

Cell viability assay
Cells were seeded into 96-well plates. Twenty-four hours after seeding, cells were treated with indicated drugs for 2 hours. Subsequently, drugs were removed by extensive washing and cultured for an additional 72 hours. Cell viability was measured using a CellTiter-Blue viability assay (Promega). Relative survival was normalized to the untreated control and corrected for background signal.

Flow cytometry for measuring drug uptake in cells
Cells were treated with 1μM of the indicated compounds for 2 hours. Samples were washed, collected and fixed with paraformaldehyde. Samples were analyzed by flow cytometry using BD FACS aria II, with 561 nm laser and 610/20nm detector. Data was analyzed using FlowJo software.

Quantification and statistical analysis
Each experiment was assayed in triplicate, unless stated otherwise. All error bars denote SD. Statistical analyses was performed using Prism 8 software (GraphPad Inc.). Two-tailed Pearson analysis was used to determine correlations, ns, not significant, $*p = < 0.05$, $**p = < 0.01$.

‡ The stereochemical outcome of the glycosylations indicates that long-range participation of the *N*-Alloc group does not play a significant role in the studied glycosylations [30,31].

ACKNOWLEDGEMENTS
This work was supported by grants from the Dutch Cancer Society KWF (JN) and by the Institute for Chemical Immunology, an NWO Gravitation project funded by the Ministry of Education, Culture and Science of the Netherlands to HO and JN.

CONFLICTS OF INTEREST
J. Neefjes is a shareholder in NIHM that aims to produce aclarubicin for clinical use.

REFERENCES
1 Grand View Research (2016) Doxorubicin Market By Application (Ovarian, Multiple Myeloma, Kaposi Sarcoma, Leukemia, Bone Sarcoma, Breast, Endometrial, Gastric, Liver, Kidney, Other Cancers) And Segment Forecasts, 2018 - 2024.
2 Lefrak EA, Pit'ha J, Rosenheim S & Gottlieb JA (1973) A clinicopathologic analysis of adriamycin cardiotoxicity. Cancer 32, 302–314.
3 Krohn K (2008) Anthracycline Chemistry and Biology I Biological Occurence and

Biosynthesis, Synthesis and Chemistry (H. Balzani, V.; de Meijere, A.; Houk, K. N.; Kessler, H.; Lehn, J.-M.; Ley, S.V.; Schreiber, S. L.; Thiem, J.; Trost, B.M. ; Vögtle, F.; Yamamoto, ed.) Springer Verlag.
4 Weiss RB (1992) The anthracyclines: will we ever find a better doxorubicin? Semin Oncol 19, 670–686.
5 Booser DJ & Hortobagyi GN (1994) Anthracycline Antibiotics in Cancer Therapy. Drugs 47, 223–258.
6 Mele D, Nardozza M, Spallarossa P, Frassoldati A, Tocchetti CG, Cadeddu C, Madonna R, Malagù M, Ferrari R & Mercuro G (2016) Current views on anthracycline cardiotoxicity. Heart Fail Rev 21, 621–634.
7 Launchbury AP, Habboubi N, Paul Launchbury A, Habboubi N, Launchbury AP & Habboubi N (1993) Epirubicin and doxorubicin: a comparison of their characteristics, therapeutic activity and toxicity. Cancer Treat Rev 19, 197–228.
8 Nitiss JL (2009) Targeting DNA topoisomerase II in cancer chemotherapy. Nat Rev Cancer 9, 338–350.
9 Pang B, Qiao X, Janssen L, Velds A, Groothuis T, Kerkhoven R, Nieuwland M, Ovaa H, Rottenberg S, van Tellingen O, Janssen J, Huijgens P, Zwart W & Neefjes J (2013) Drug-induced histone eviction from open chromatin contributes to the chemotherapeutic effects of doxorubicin. Nat Commun 4, 1–13.
10 Qiao X, van der Zanden SY, Wander DPA, Borràs DM, Song J-Y, Li X, van Duikeren S, van Gils N, Rutten A, van Herwaarden T, van Tellingen O, Giacomelli E, Bellin M, Orlova V, Tertoolen LGJ, Gerhardt S, Akkermans JJ, Bakker JM, Zuur CL, Pang B, Smits AM, Mummery CL, Smit L, Arens R, Li J, Overkleeft HS & Neefjes J (2020) Uncoupling DNA damage from chromatin damage to detoxify doxorubicin. Proc Natl Acad Sci 117, 15182–15192.
11 Pang B, de Jong J, Qiao X, Wessels LFA & Neefjes J (2015) Chemical profiling of the genome with anti-cancer drugs defines target specificities. Nat Chem Biol 11, 472–480.
12 Wander DPA, van der Zanden SY, van der Marel GA, Overkleeft HS, Neefjes J & Codée JDC (2020) Doxorubicin and Aclarubicin: Shuffling Anthracycline Glycans for Improved Anticancer Agents. J Med Chem 63, 12814–12829.
13 Kulikowski T, Bretner M, Najda A & Cova L (2006) New Derivatives of Epirubicin, their Medicinal Application and Pharmaceuticaly Acceptable Forms of Drugs. .
14 Arlandini, Vigevani & Arcamone (1980) Interaction of new derivatives of daunorubicin and doxorubicin with DNA. Part II. Farm Ed Sci 35, 65–78.
15 Yu B (2018) Gold(I)-Catalyzed Glycosylation with Glycosyl o -Alkynylbenzoates as Donors. Acc Chem Res 51, 507–516.
16 Wander DPA (2019) Understanding Anthracyclines: Synthesis of a Focused Library of Doxorubicin/Aclarubicin - Inspired Structures. .
17 Fan E, Shi W & Lowary TL (2007) Synthesis of Daunorubicin Analogues Containing Truncated Aromatic Cores and Unnatural Monosaccharide Residues. J Org Chem 72, 2917–2928.
18 Noshita T, Sugiyama T, Kitazumi Y & Oritani T (1995) Reinvestigation of Phenolic Ferrier Reaction: Selective Synthesis of Aryl O-Δ 2 -Glycosides. Biosci Biotechnol Biochem 59, 2052–2055.
19 Ma Y, Li Z, Shi H, Zhang J & Yu B (2011) Assembly of digitoxin by gold(I)-catalyzed glycosidation of glycosyl o-alkynylbenzoates. J Org Chem 76, 9748–9756.
20 Renneberg B, Li Y-M, Laatsch H & Fiebig H-H (2000) A short and efficient transformation of rhamnose into activated daunosamine, acosamine, ristosamine and epidaunosamine derivatives, and synthesis of an anthracycline antibiotic acosaminyl-ε-

iso-rhodomycinone. Carbohydr Res 329, 861–872.
21 Horton D & Weckerle W (1975) A preparative synthesis of 3-amino-2,3,6-trideoxy-l-lyxo-hexose (daunosamine) hydrochloride from d-mannose. Carbohydr Res 44, 227–240.
22 Hansen T, Lebedel L, Remmerswaal WA, van der Vorm S, Wander DPA, Somers M, Overkleeft HS, Filippov D V., Désiré J, Mingot A, Bleriot Y, van der Marel GA, Thibaudeau S & Codée JDC (2019) Defining the SN1 Side of Glycosylation Reactions: Stereoselectivity of Glycopyranosyl Cations. ACS Cent Sci 5, 781–788.
23 Romero JAC, Tabacco SA & Woerpel KA (2000) Stereochemical Reversal of Nucleophilic Substitution Reactions Depending upon Substituent: Reactions of Heteroatom-Substituted Six-Membered-Ring Oxocarbenium Ions through Pseudoaxial Conformers. J Am Chem Soc 122, 168–169.
24 Ayala L, Lucero CG, Romero JAC, Tabacco SA & Woerpel KA (2003) Stereochemistry of Nucleophilic Substitution Reactions Depending upon Substituent: Evidence for Electrostatic Stabilization of Pseudoaxial Conformers of Oxocarbenium Ions by Heteroatom Substituents. J Am Chem Soc 125, 15521–15528.
25 Zeng J, Sun G, Yao W, Zhu Y, Wang R, Cai L, Liu K, Zhang Q, Liu X-W & Wan Q (2017) 3-Aminodeoxypyranoses in Glycosylation: Diversity-Oriented Synthesis and Assembly in Oligosaccharides. Angew Chemie Int Ed 56, 5227–5231.
26 Garro-Helion F, Merzouk A & Guibé F (1993) Mild and selective palladium(0)-catalyzed deallylation of allylic amines. Allylamine and diallylamine as very convenient ammonia equivalents for the synthesis of primary amines. J Org Chem 58, 6109–6113.
27 Bartner P, Boxler DL, Brambilla R, Mallams AK, Morton JB, Reichert P, Sancilio FD, Surprenant H, Tomalesky G, Lukacs G, Olesker A, Thang TT, Valente L & Omura S (1979) The megalomicins. Part 7. A structural revision by carbon-13 nuclear magnetic resonance and X-ray crystallography. Synthesis and conformational analysis of 3-dimethylamino- and 3-azido- D - and - L -hexopyranosides, and the crystal structure of 4″-O-(4-Iodobenzoyl)megalomicin A. J Chem Soc, Perkin Trans 1 0, 1600–1624.
28 Kuo LJ & Yang LX (2008) γ-H2AX- A novel biomaker for DNA double-strand breaks. In Vivo (Brooklyn) 22, 305–310.
29 Olive PL, Wlodek D & Banáth JP (1991) DNA double-strand breaks measured in individual cells subjected to gel electrophoresis. Cancer Res 51, 4671–6.
30 Hansen T, Elferink H, van Hengst JMA, Houthuijs KJ, Remmerswaal WA, Kromm A, Berden G, van der Vorm S, Rijs AM, Overkleeft HS, Filippov D V, Rutjes FPJT, van der Marel GA, Martens J, Oomens J, Codée JDC & Boltje TJ (2020) Characterization of Glycosyl Dioxolenium Ions and Their Role in Glycosylation Reactions. Nat Commun 11, 1–9.
31 Komarova BS, Tsvetkov YE & Nifantiev NE (2016) Design of α-Selective Glycopyranosyl Donors Relying on Remote Anchimeric Assistance. Chem Rec 16, 488–506.

SUPPLEMENTAL INFORMATION

5

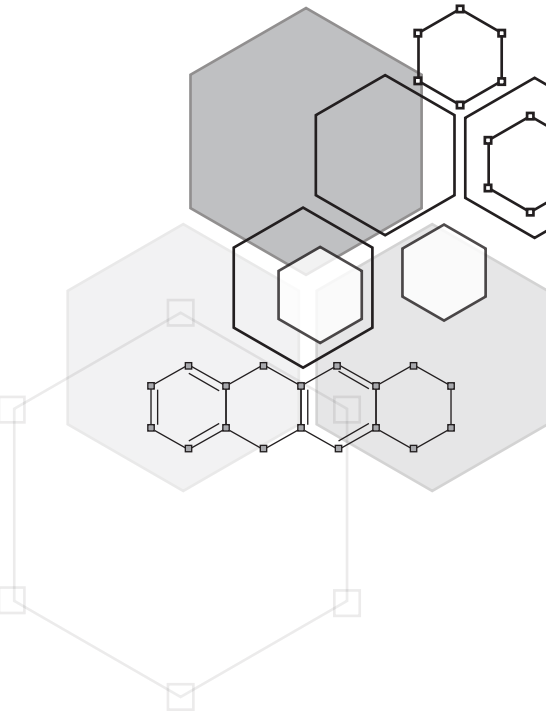

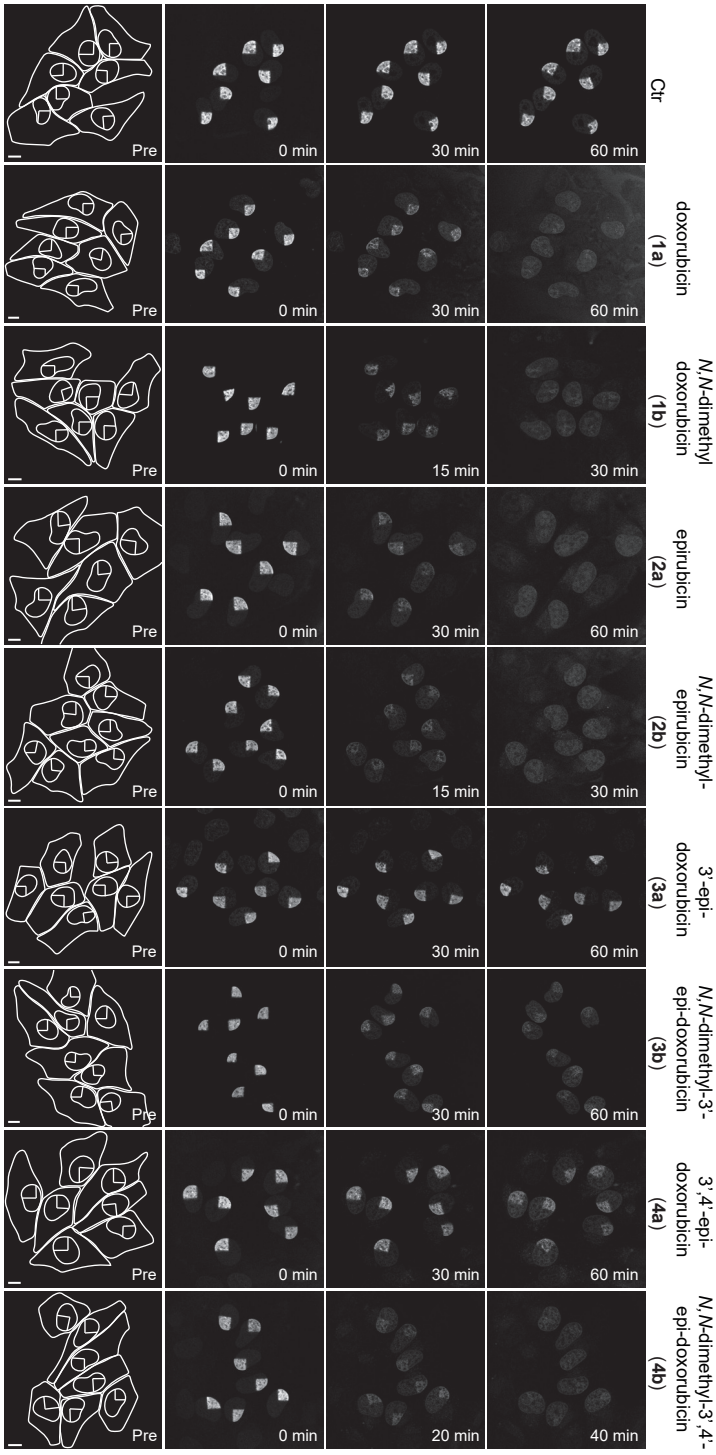
Ctr
doxorubicin (1a)
N,N-dimethyl doxorubicin (1b)
epirubicin (2a)
N,N-dimethyl-epirubicin (2b)
3'-epi-doxorubicin (3a)
N,N-dimethyl-3'-epi-doxorubicin (3b)
3',4'-epi-doxorubicin (4a)
N,N-dimethyl-3',4'-epi-doxorubicin (4b)
Pre
0 min
15 min
20 min
30 min
40 min
60 min

Figure S1. Chromatin damage is induced by the different doxorubicin isomers. *Part of the nucleus of MelJuso cells stably expressing PAGFP-H2A was photo-activated and histone eviction was measured by time-lapse confocal microscopy upon administration of 10μM of the indicated compounds. Lines in the left panel define the cytoplasm, nucleus and activated region of the nucleus before treatment. Stills at indicated time points from time-lapse experiment are shown. Scale bar, 10μm*

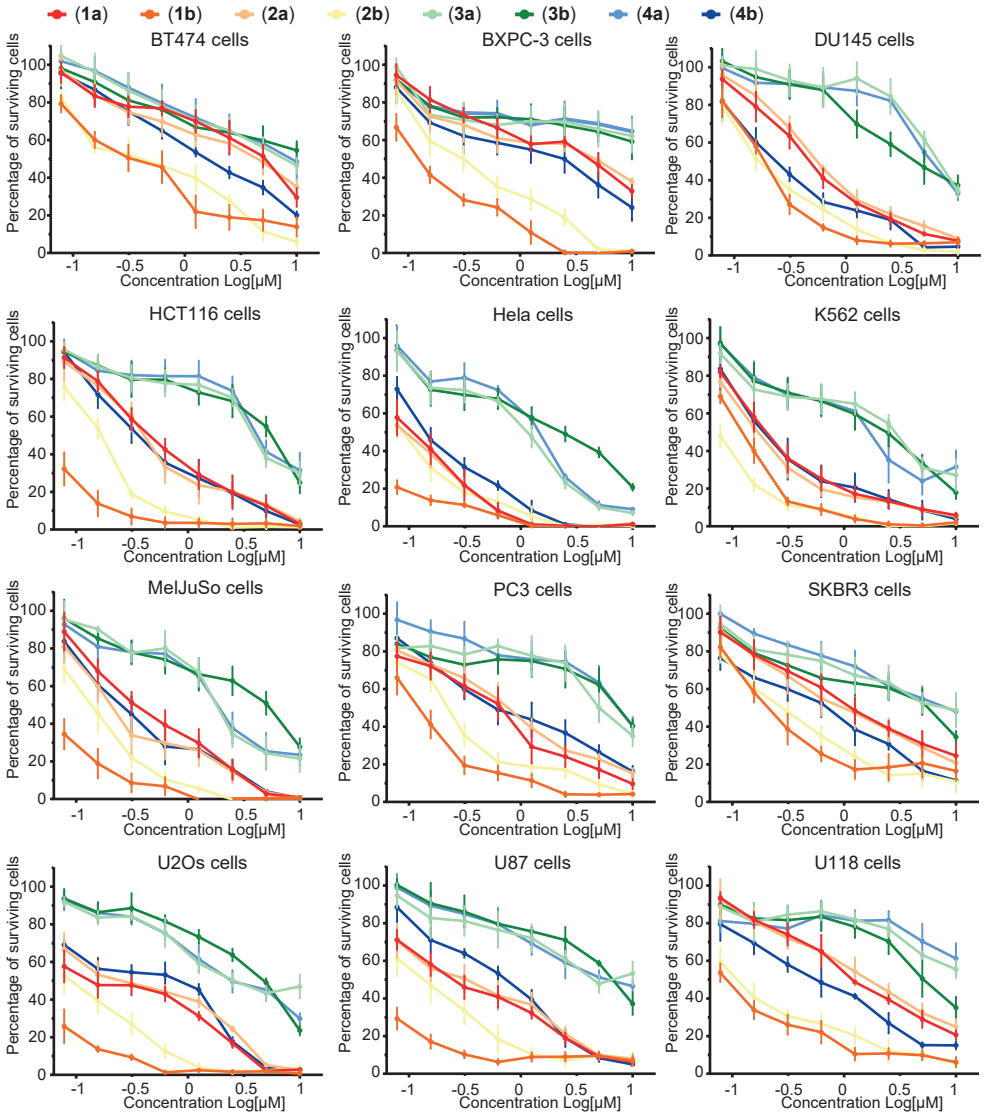

Figure S2. Cytotoxic effect in different tumor cell lines of the doxorubicin isomers. *Indicated tumor cells were treated for 2 hours with different doses of the indicated doxorubicin isomers followed by drug removal. Cell viability was measured by a CellTiter-Blue assay 72 hours post treatment. Data is shown as mean ± SD from four different experiments.*

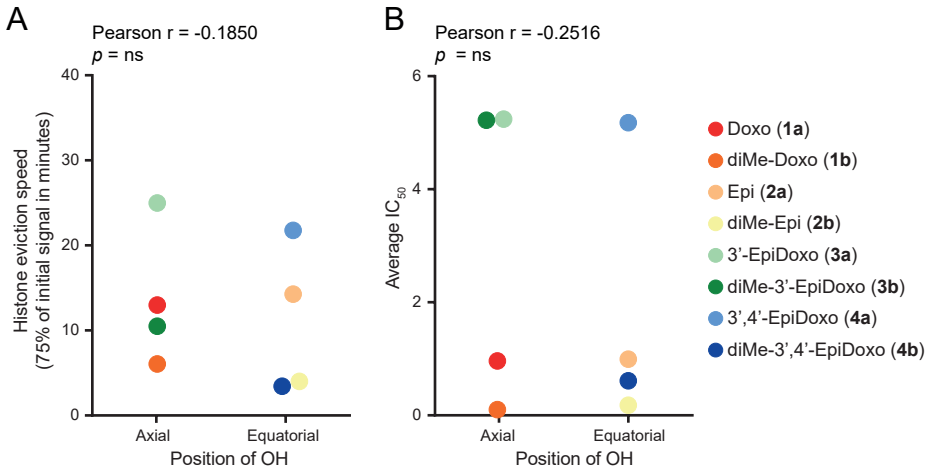

Figure S3. The position of the OH has little effect on the effectivity of the doxorubicin isomers. *(A and B) The position of the hydroxyl group of the doxorubicin isomers was correlated with the rate of histone eviction (A) and cytotoxicity (B). Two-tailed Pearson r correlation ns; not significant.*